Dyes and Pigments 89 (2011) 330–335

Contents lists available at ScienceDirect

Dyes and Pigments

journal homepage: www.elsevier.com/locate/dyepig

New water-soluble dicyano-stilbene dyes: One and two-photon fluorescence and photo-response to BSA

Jingqiang Cui, Jiangli Fan, Xiaojun Peng*, Shiguo Sun

State Key Laboratory of Fine Chemicals, Dalian University of Technology, 158 Zhongshan Road, Dalian 116012, PR China

ARTICLE INFO

Article history:
Received 7 December 2009
Received in revised form
12 September 2010
Accepted 17 September 2010
Available online 26 September 2010

Keywords:
Fluorescence
Dye
Two-photon absorption action cross section
Molecular switch
Bovine serum albumin
Stainer

ABSTRACT

Two novel quadrapolar stilbene fluorescent dyes with CN groups (DCNs) are reported. Photophysical properties such as fluorescence, intermolecular charge transfer, two-photon absorption action cross section ($\delta\Phi$) and fluorescence-response to bovine serum albumin (BSA) are investigated and discussed. The fluorescence emission is red-shifted and quenched with the increase in polarity of solvents. In aqueous buffer (pH 7.0), compound **1b** has a large blue shift (74 nm) and 37-fold fluorescence enhancement when interacts with BSA. The response is noticeable by naked eyes. Cations, anions and DNA have no such responses. It is resulted from the change of environmental polarity from aqueous solution to hydrophobic cage in protein, and sequentially, the change in the effect of excited intermolecular charge transfer.

1. Introduction

Protein-responsive fluorophores [1–5] and chromophores are of scientific and practical interest to detect various proteins such as bovine serum albumin (BSA) [6–8]. There are two ways to label proteins with an fluorophore: one is covalent labeling, requiring a reactive functional group on the label molecule to react to the proteins; and another is noncovalent labeling, whereby the probe forms a complex with the proteins via noncovalent interactions, such as ionic, electrostatic, hydrophobic, and hydrogen bonding. The noncovalent labeling method is typically a simpler and faster protocol compared to conventional covalent labeling [9,10].

Recently, fluorophores with two-photon excited fluorescence (TPEF), which are based on molecular two-photon absorption (TPA), have received increasing interest for its various advantages such as localized excitation, increased penetration depth, lower tissue autofluorescence and self-absorption, in addition to the reduced photodamage and photobleaching [11,12]. A useful fluorophore for such applications should have a large TPA cross-section, δ, in NIR–IR region, appreciable solubility in water, high photostability, and sensitive fluorescence-enhancement to special biological substrates.

Meantime, various organic TPEF compounds with high quantum yields, large TPA cross sections δ, and good stability have been reported [13–18]. Especially, the CN groups in the molecular core increases the δ values significantly [18]. Whereas, few of the stilbene derivatives containing CN groups are water-soluble [19,20]. The water-solubility is very important for practical applications for protein determinations.

Herein we report the synthesis, photophysics, and protein-responsive properties of water-soluble stilbene derivatives with CN groups (DCNs) (Fig. 1): there is a 37-fold fluorescence enhancement of DCN **1b** after interaction with BSA.

2. Experiments

2.1. Materials and general methods

Deionized water was redistilled before use. All the solvents were of analytical grade. ^{1}H NMR and ^{13}C NMR spectra were recorded on a VARIAN INOVA-400 spectrometer with chemical shifts reported as ppm (in $CDCl_3$, TMS as internal standard). Mass spectrometric data were obtained on a HP1100LC/MSD MS spectrometer and a LC/Q-Tof MS spectrometer. Fluorescence measurements were performed on a PTI-700 Felix and Time-Master system, and the slit width was 5 nm for both excitation and emission. Absorption spectra were measured on Lambda 35 UV/vis spectrophotometer.

* Corresponding author. Tel.: +86 0411 39893899; fax: +86 0411 39893800.
E-mail address: pengxj@dlut.edu.cn (X. Peng).

0143-7208/$ – see front matter © 2010 Elsevier Ltd. All rights reserved.
doi:10.1016/j.dyepig.2010.09.005

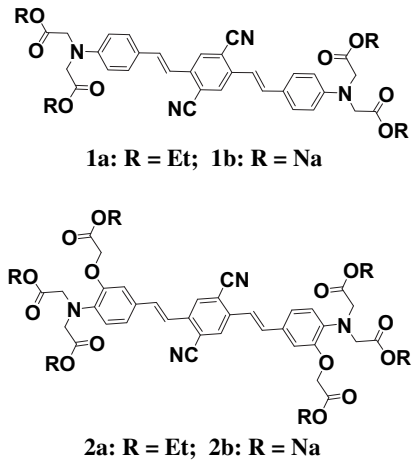

Fig. 1. New stilbene derivatives with CN groups (DCNs).

All pH measurements were made with a Model PHS-3C meter. Melting points were determined by an X-6 micro-melting point apparatus and are uncorrected. The fluorescence quantum yields of DCNs were measured using standard methods on air-equilibrated samples at room temperature. Quinine bisulfate in 0.05 mol L^{-1} H_2SO_4 solution ($\Phi = 0.546$) was used as a reference [21]. TPEF spectra were measured on SD2000 spectrometer (Ocean Optical). The TPA cross sections (δ_{TPA}) of DCNs were determined by the two-photon-induced excited fluorescence method [22].

2.2. Synthesis

The synthetic routes for DCNs are shown in Fig. 2.

2.2.1. Compound *1a*

Aldehyde **3** [23,24] (0.29 g, 1 mmol), and NaH (130 mg, 5.4 mmol) were dissolved in THF (3 mL), and the solution was cooled to 0 °C under N_2. To this solution, phosphonate **5** [25] (1.46 g, 5.0 mmol) in THF (9 mL) was added dropwise. The reaction mixture was stirred for 1 h at 0 °C, and then for 12 h at room temperature, followed by the removal of THF under reduced pressure. Water then was added to the reaction mixture, and the product was extracted with dichloromethane (4 × 100 mL). The organic layer was dried with dry Na_2SO_4 followed by evaporation of the solvent. The crude product was separated by column chromatography with a gradient of hexane in dichloromethane (20–0%) and ethyl acetate in dichloromethane (0–20%). Compound **1a** (296 mg, 32%) yielded as a yellow powder. M.p. 194.3–195.4 °C. ^{1}H NMR ($CDCl_3$, 400 MHz) δ: 7.96 (s, 2H), 7.47 (d, J = 8.4 Hz, 4H), 7.21(d, J = 16.0 Hz, 2H), 7.15 (d, J = 16.0 Hz, 2H), 6.63 (d, J = 8.4 Hz, 4H), 4.26 (s, 8H), 4.25–4.17 (m, 8H), 1.30 (t, J = 8.0 Hz, 12H). ^{13}C NMR ($CDCl_3$, 100 MHz) δ: 171.132, 168.732, 149.535, 141.166, 138.786, 134.468, 129.598, 122.674, 119.952, 119.335, 116.849, 114.794, 113.329, 77.517, 77.199, 76.881, 66.465, 61.523, 61.029, 53.974, 14.388. TOF MS (ES): m/z Calcd for [M^+], $C_{40}H_{42}N_4O_8$, 706.2998, Found: 729.3000.

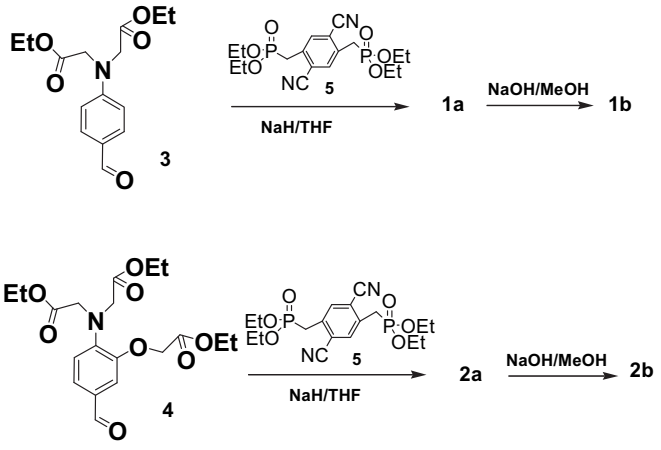

Fig. 2. Synthetic procedures of DCNs.

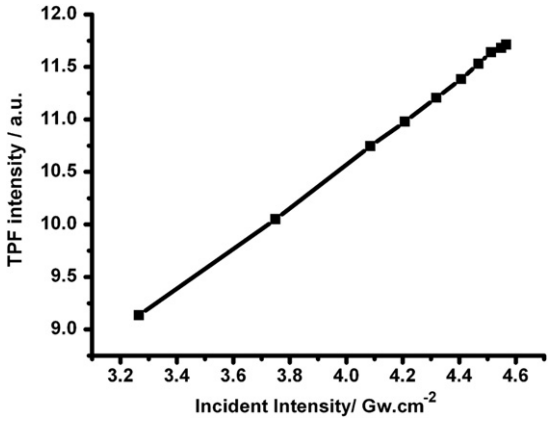

Fig. 3. The dependence of the up-converted fluorescence intensity for **1b** in H_2O on the incident intensity.

2.2.2. Compound *2a*

Aldehyde **4** [23,24] (0.38 g, 1 mmol), and NaH (130 mg, 5.4 mmol) were dissolved in THF (3 mL), and the solution was cooled to 0 °C under N_2. To this solution, phosphonate **5** (1.46 g, 5.0 mmol) in THF (9 mL) was added dropwise. The reaction mixture was stirred for 1 h at 0 °C, and then for 12 h at room temperature, followed by the removal of THF under reduced pressure. Water then was added to the reaction mixture, and the product was extracted with dichloromethane (4 × 100 mL). The organic layer was dried with dry Na_2SO_4 followed by evaporation of the solvent. The crude product was separated by column chromatography with a gradient of hexane in dichloromethane (20–0%) and ethyl acetate in dichloromethane (0–20%). Compound **2a** (326 mg, 35%) yielded

Table 1
Photophysical properties of DCNs in various solvents.

Dye	Solvent[a]	λ^{abs}_{max}[b] /nm	λ^{OP}_{max}[b] /nm	Stokes shift/nm	Φ[c]	λ^{TP}_{max}[d] /nm	$\Phi\delta_{max}$[e]
1b	1,4-dioxane	392	510	118	0.61	820	601
	$CHCl_3$	397	527	130	0.52	820	357
	THF	392	542	150	0.48	820	291
	MeCN	396	565	169	0.43	820	251
	DMSO	407	567	160	0.11	820	189
	H_2O	377	583	206	0.04	820	57
	1,4-dioxane	354	455	101	0.45	830	259
	$CHCl_3$	360	460	100	0.33	850	189
	THF	363	461	98	0.25	730	157
2b	MeCN	378	462	84	0.12	720	112
	DMSO	388	473	85	0.09	850	89
	H_2O	353	462	109	0.06	720	62

[a] The numbers in the parenthesis are normalized empirical parameter of solvent polarity.
[b] λmax of the absorption and emission spectra in nm.
[c] Fluorescence quantum yields, ±15%.
[d] λmax of the two-photon excitation spectra in nm.
[e] Two-photon action cross section (10^{-50} cm^4s/photon GM), ±15%.

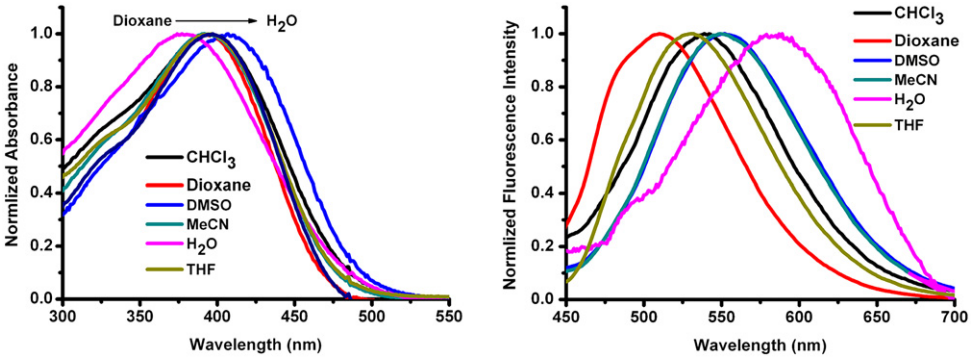

Fig. 4. One-photon absorption (left), emission spectra (right) of **1b** (10 μmol L^{-1}).

as a yellow powder. M.p. 184.3–185.4 °C. ^{1}H NMR ($CDCl_3$, 400 MHz) δ: 7.97 (s, 2H), 7.20 (d, J = 16.4 Hz, 2H), 7.17 (s, 2H), 7.16 (d, J = 8.0 Hz, 2H), 6.88 (d, J = 16.0 Hz, 2H), 6.86 (d, J = 8.4 Hz, 2H), 4.69 (s, 8H), 4.31 (s, 4H), 4.29–4.17 (m, 12H), 1.29 (t, J = 8.0 Hz, 18H). ^{13}C NMR ($CDCl_3$, 100 MHz) δ: 171.132, 168.732, 149.535, 141.166, 138.786, 134.468, 129.598, 122.674, 119.952, 119.335, 116.849, 114.794, 113.329, 77.517, 77.199, 76.881, 66.465, 61.523, 61.029, 53.974, 14.388. TOF MS (ES): m/z Calcd for [M^+], $C_{48}H_{54}N_4O_{14}$, 933.3534, Found: 933.3537.

2.2.3. Compound *1b* and *2b*

Solution of the ester **1a** was saponified under basic conditions to generate free **1b** using a standard protocol [26]. In all cases, a suspension of the ester (60 mg, 0.049 mmol) and NaOH (120 mg, 3 mmol) in methanol was refluxed overnight under nitrogen, at which time TLC analysis showed complete consumption of starting material and was kept into the freezer. The precipitate formed was filtered and washed with cold methanol and hexane. Solids obtained were completely soluble in water and was directly used to prepare stock solutions in Millipore water for further spectroscopic measurements.

1b. Yellow solid. Yield: 95 %. M.p. 235.5–236.6 °C. TOF MS (ES): m/z Calcd. for $C_{32}H_{26}N_4O_8$ 594.1832, Found: 594.1834.

2b. Yellow solid. Yield: 92 %. M.p. 215.3–216.4 °C. TOF MS (ES): m/z Calcd. for $C_{36}H_{30}N_4O_{14}$ 742.1759, Found: 742.1762.

2.3. Determination of quantum yield

The relative quantum yields of DCNs were determined by using Quinine bisulfate in 0.05 mol L^{-1} H_2SO_4 solution (Φ = 0.546) as the standard and were calculated through the following equation [27]:

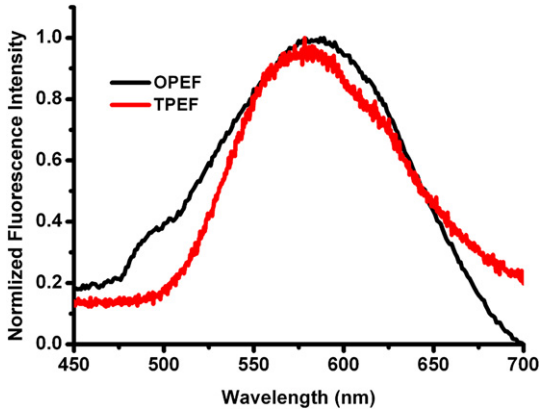

Fig. 5. OPEF and TPEF spectra of **1b** in water. OP Excitation: 380 nm, TP Excitation: 820 nm.

$$\Phi_u = \Phi_s F_u A_s \lambda_{exs} \eta_u / F_s A_u \lambda_{exu} \eta_{us}$$

where Φ is quantum yield; F is integrated area under the corrected emission spectra; A is absorbance at the excitation wavelength; λ_{ex} is the excitation wavelength; η is the refractive index of the solution; the subscripts u and s refer to the unknown and the standard, respectively.

2.4. Spectroscopic measurements

Stock solutions of DCNs were prepared in DMSO and the OP absorption and emission spectra (OPEF) were obtained in different solvent. For absorption spectra of the BSA-responsive measurements, sample solutions were obtained by mixing appropriate amount of stock solution of DCNs (1 mmol L^{-1} in DMSO) and phosphate buffer (20 mmol L^{-1}) in water and finally diluted with buffer to make the solution having desired concentrations of DCNs. OPEF measurements were carried out similarly. TPEF spectra were recorded on SD2000 spectrometer (Ocean Optical) with excitation by using a femtosecond laser (Tsunami, Spectra-Physics) with 70-fs pulse width and 80 MHz repetition rate.

2.5. Measurement of TPA cross section

The TPA cross sections of the DCNs were determined by the two-photon-induced excited fluorescence method. And it is assumed that the quantum efficiencies after two-photon excitation are the same as those after one-photon excitation. The TPA cross sections are obtained by calibration against fluorescein with known δ value in aqueous NaOH solution (pH = 11) at concentrations of 1.0×10^{-4} mol·L^{-1} for the femtosecond measurement. The samples were dissolved in solvents at concentrations of 1.0×10^{-4} mol L^{-1}. The error of TPEF measurement is about 15%. To ensure that the measured signals were solely due to TPA, the dependence of TPEF on the incident intensity was verified in each case to be quadratic. The slope is approximately two (Fig. 3). Therefore, this is a two-photon absorption process.

2.6. BSA-responsive properties of the DCNs in PBS buffer solutions

A series of PBS buffer solutions (20 mmol L^{-1}, pH 7.0) containing various amounts of BSA (0 ~ 20 μmol L^{-1}) and 10 μmol L^{-1} of DCNs were prepared. The emission spectra of the dyes were recorded with increasing concentration of the BSA.

2.7. Interferences to the fluorescence response of BSA

To explore further the utility of **1b** as a fluorescence probe for BSA, the interference experiments were conducted including

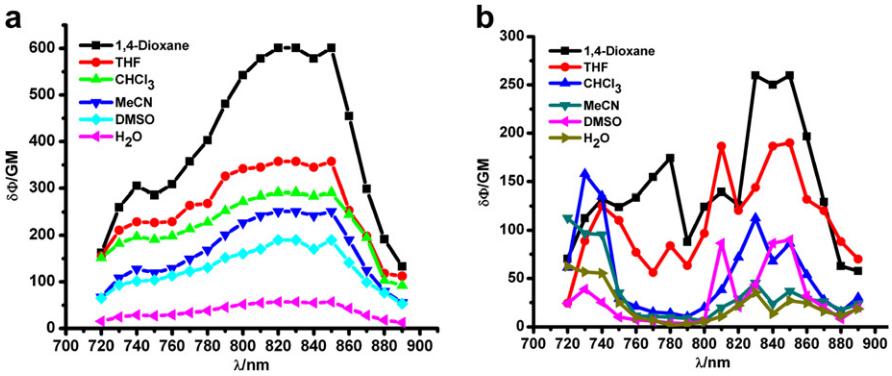

Fig. 6. Two-photon action spectra of DCNs: a (**1b**), b (**2b**). TP Excitation: 720–890 nm.

various metal cations, anions and DNA (calf thymus) in PBS buffer solutions.

2.8. Investigation of the pH dependency of 1b-BSA

The fluorescence responses of **1b**-BSA were investigated in three different pH buffer solutions.

3. Results and discussion

3.1. Spectral properties

3.1.1. One-photon absorption and emission spectra of DCNs

The photo-physical properties of DCNs in different solvents are summarized in Table 1. The OPEF spectra show large red-shift with solvent polarity (Π^*) [28] in the order: 1,4-dioxane < $CHCl_3$ < THF < MeCN < DMSO < H_2O. For example, the OPEF spectrum of **1b** in aqueous solution is red-shifted for 73 nm to the one in dioxane, although the absorption has small blue-shifts (Fig. 4). It implies that there are great changes in the molecular geometry of excited states before fluorescence emission. On the other hand, the quantum yield (Φ) of **1b** in aqueous solution is much quenched (from 0.61 in dioxane to 0.04 in water). These photo-physical data indicate that DCNs can take place an ICT phenomenon between the fluorophore center and the amino group. Their high sensitivity to polarity change of environments should benefit for DCNs as fluorescent sensors.

3.1.2. Two-photon excited fluorescence (TPEF) spectra of DCNs

The TPEF spectra of DCNs were obtained with excitation at 830 nm by using a mode-locked Ti/sapphire femtosecond laser in the different organic solvents. For a certain compound, the spectral profiles and peak positions of OPEF and TPEF are basically the same. Although TPEF wavelength has a small blue shift relative to the OPEF spectrum of dye **1b**, the vibronic structures in the OPEF and TPEF spectra are very similar in water (Fig. 5). This implies that OPEF and TPEF come from the same fluorescent excited state. The TPEF emission peak at 485 nm is weaker in comparison with the profile of the OPEF spectrum. This is due to the higher concentration (1.0×10^{-4} mol L^{-1}) of **1b** used for TPEF determination, and the fluorescence quantum yield (Φ) of **1b** in aqueous solution is so small that the excitation efficiency of TPEF in water is much low.

3.2. TPA cross section

The TPA cross sections δ_{TPA} were determined by using the two-photon-induced fluorescence measurement technique. To avoid possible complications due to the excited-state excitation, we have used a mode-locked Ti/sapphire femtosecond (fs) laser pulses. The pulse width and repetition rate of the laser are 70 fs and 80 MHz, respectively. The values $\delta\Phi_{TPA}$ of DCNs decrease with the change in the solvents from 1,4-dioxane toH_2O. For example, $\delta\Phi_{TPA}$ of **1b** reduce gradually from 601 GM (in 1,4-dioxane) to 57 GM (in H_2O) (Fig. 6), which should be attributed to the excited state charge transfer. More polar solvent H_2O is favorable to balance positive and negative charge arising from excited state, which will then be efficiently deactivated, so the values of $\delta\Phi_{TPA}$ of the dyes in H_2O are comparatively small. Significant decreases in $\delta\Phi_{TPA}$ of other dye systems with increased solvent polarity have been reported in literatures [29]. For practical applications, TP cross section per molecular weight (δ_{max}/MW) is more valuable. The δ_{max}/MW of **1b** is 2.39 in H_2O solvent. Generally, δ_{max}/MW > 1.0 have been found to

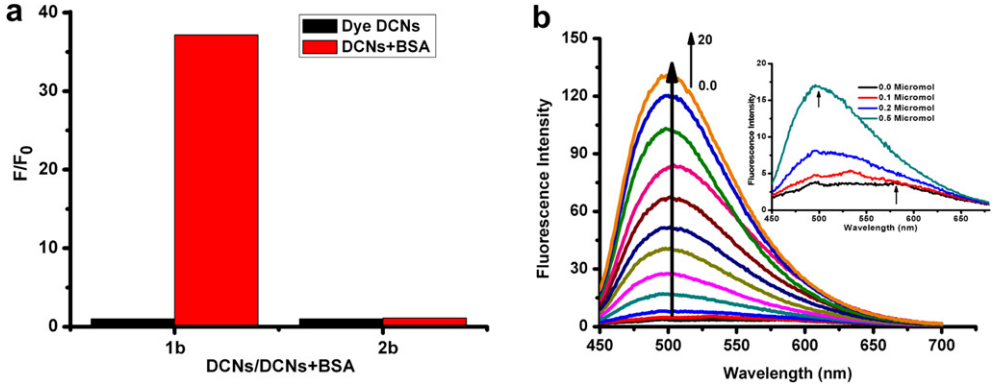

Fig. 7. a. Ratio of fluorescence intensity (**1b**: F/F_0 at 501 nm, **2b**: F/F_0 at 467 nm) of 10 μmol L^{-1} dye DCNs in the presence of BSA (2 μmol L^{-1}). b. Fluorescence spectra of 10 μmol L^{-1} dye **1b** binding with BSA in PBS buffer solutions (pH 7.0) at room temperature. Excitation: 380 nm.

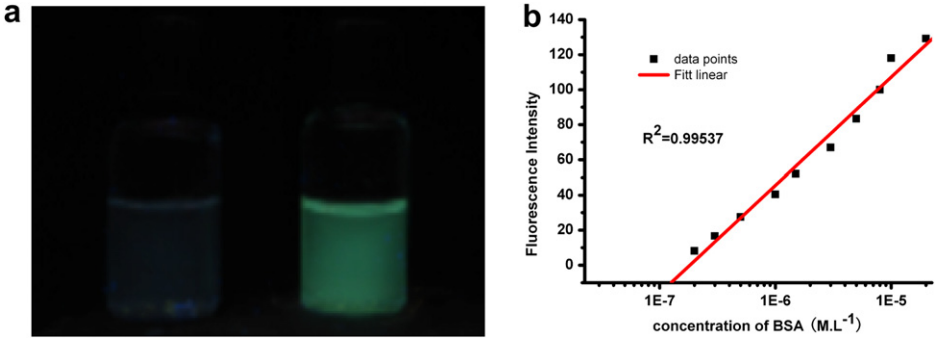

Fig. 8. a. Photographs of compound **1b** solutions in the absence (left) and the presence (right) of BSA. b. plot of the fluorescence intensity at 501 nm as a function of BSA concentration.

be good for such applications [30,31]. So, the intensity of the TPF of **1b** is strong enough for practical applications, although TPA action cross section is not very high.

3.3. Fluorescence off-on response of DCNs to BSA in aqueous solutions

When BSA is added into the PBS buffer solution of **1b** (pH 7.0), great fluorescence enhancements are observed (Fig. 7b). As **1b** has a very weak emission in water ($\Phi = 0.04$) by itself, the switching-on effect of BSA is rather acute. Adding 20 μmol L^{-1} of BSA, c.a. 37-fold enhancement in fluorescence ($\Phi = 0.36$) is obtained. The fluorescence intensity is linearly increased with BSA concentration up to 20 μmol L^{-1} ($R^2 > 0.995$, Fig. 8b). And obvious emission blue-shifts (from 575 to 501 nm) are companied with the off-on process. This significant fluorescence turn-on leads to visual observation of fluorescence by naked eye from dark to bright green (Fig. 8a). The fluorescence responses of **1b** to BSA are very close to effects of the polarity change of solvents from water to dioxane (Table 1). Therefore, the **1b**-BSA interaction should be resulted from a great change in the environments of **1b** from hydrophilic (polar) aqueous solution to hydrophobic (apolar) cage of BSA. Under identical conditions, no such kind of fluorescence response is observed in the cases of **2b** (Fig. 7a). Although **2b** is soluble in water, compared with **1b**, it has a branching molecular structure which hinders the molecule get into the hydrophobic cage of BSA.

3.4. Interferences to the fluorescence response of BSA

Compound **1b**, with multi-carboxyl groups, like a chelating agent, might interact with multivalent metal cations (such as Ca^{2+}) under physiological conditions. This kind of interaction might let some interference of the cations to the response to proteins. Addition of various metal ions (50 equiv of Mn^{2+}, Ca^{2+}, Mg^{2+}, Zn^{2+}, Hg^{2+}, Cu^{2+} and Ni^{2+}) into **1b** (10 μmol L^{-1}) solution, however, the fluorescence intensity of **1b** has little change (Fig. 9a). The results imply that the responses of 1b to cations are not so strong. Anions (50 equiv of NO_3^-, NO_2^-, HCO_3^-, CO_3^{2-}, HPO_4^{2-}, PO_4^{3-}, SO_4^{2-}, HSO_3^-, SO_3^{2-}, SCN^-, Cl^-, Br^-, I^-, and F^-) and DNA (calf thymus) also show nearly no changes in fluorescence intensity of **1b** in PBS buffer (pH 7.0) solution (Fig. 9b). Generally speaking, the selectivity between a protein and a DNA is a difficulty for a staining dye based on the polarity of environment, as hydrophobic properties in both kinds of bio-macromolecules are similar. The independence of **1b** to DNA might be from the nonspecific electrostatic repulsion between the anionic carboxylated groups of **1b** and the polyanionic phosphate backbone of DNA. It is this kind of repulsion that would reduce binding affinity for **1b** and DNA.

3.5. Investigation of the pH dependency of *1b*-BSA

We also examined the pH dependency of the emissive properties of **1b** binding with BSA by addition of different pH buffer solution (pH = 4.00 Na_2HPO_4/citric acid, pH = 7.00 PBS and pH = 9.18 boric acid). The addition of BSA showed some fluorescence enhancement in Na_2HPO_4/citric acid buffer (pH 4.00), although much greater fluorescence enhancements were achieved upon titrating the **1b** with BSA in PBS (pH 7.00) and boric acid (pH 9.18) buffers. In all cases, the fluorescence enhancement increased as more BSA was added (Fig. 10).

It is known that BSA undergoes reversible conformational isomerization with changes of pH [32]. At pH 4.00, BSA undergoes an

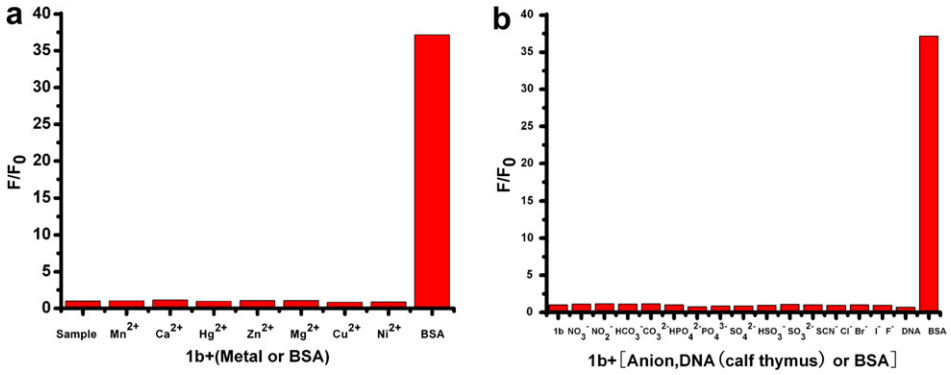

Fig. 9. Ratio of fluorescence intensity (F/F_0 at 501 nm) of 10 μmol L^{-1} dye **1b** in the presence of different metal ions (50 μmol L^{-1}) (a), anion (50 μmol L^{-1}) and DNA (100 μmol L^{-1}) (b), in PBS buffer solutions (pH 7.0) at room temperature. Excitation: 380 nm.

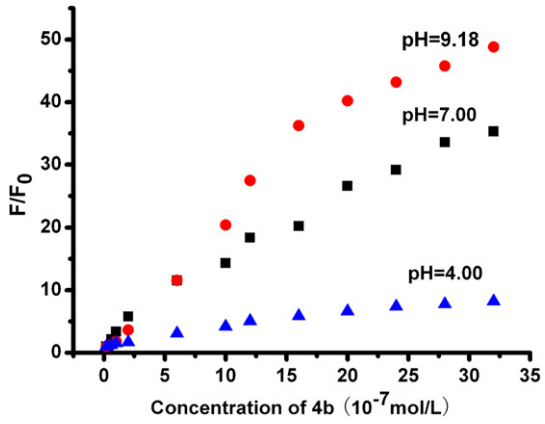

Fig. 10. Plot of the fluorescence of 10 μmol L^{-1} **1b** at 501 nm in pH 4.00, 7.00, 9.18 buffer solutions as a function of BSA concentrations (0–3.2 μmol L^{-1}). Excitation: 380 nm.

expansion with the F-E transition form, which reduces hydrophobic cage of BSA, so that the fluorescence enhancement of **1b-BSA** is lower. At pH 7.00 and 9.18 which correspond to different isomeric forms of BSA, i.e., N for the normal or native form and B for the basic form. Two kinds of BSA include much hydrophobic cage of BSA, so the interactions are the formation of a stable and non-covalent complex between **1b** and BSA and show high fluorescent enhancement.

4. Conclusion

Two water-soluble one and two-photon fluorescent dyes were synthesized. Photo-physical properties of them were investigated by the absorption, OPEF and TPEF spectra. These fluorescent dyes own the larger TPA action cross section $\delta\Phi$ in organic solution. When interacts non-covalently with BSA in aqueous solutions, new dye **1b** provides a dramatic linear-increase in the fluorescence intensity. Cations, anions and DNA have no such responses. It is resulted from the change of environmental polarity from aqueous solution to hydrophobic cage in protein, and sequentially, the change in the effect of excited intermolecular charge transfer.

Acknowledgements

This work was supported by NSF of China (207025621 and 20706008), National Basic Research Program of China (2009CB724706), Ministry of Education of China (Program for Changjiang Scholars and Innovative Reserch Team in University, IRT0711; and Cultivation Fund of the Key Scientific and Technical Innovation Project, 707016). We are also grateful to Professor Xuanming Duan and Professor Weiqiang Chen (Technical Institute of Physics and Chemistry, Chinese Academy of Science) for their help in two-photon fluorescence detection.

References

[1] Micheal Z, Wang L. Selective labeling of proteins with chemical probes in living cells. Physiology 2008;23:131–41.
[2] Nizomov N, Ismailov Z, Nizamov S, Salakhitdinova M, Tatarets A, Patsenker L, et al. Spectral-luminescent study of interaction of squaraine dyes with biological substances. Journal of Molecular Structure 2006;788:36–42.
[3] Kim J, Watson A, Henary M, Patonay G. Near-infrared cyanine dye–protein interactions. Topics in Heterocyclic Chemistry 2008;14:31–9.
[4] Meadows F, Narayanan N, Patonay G. Determination of protein–dye association by near infrared fluorescence-detected circular dichroism. Talanta 2000;50:1149–55.
[5] Suzuki Y, Yokoyama K. Design and synthesis of intramolecular charge transferbased fluorescent reagents for the highly-sensitive detection of proteins. Journal of the American Chemical Society 2005;127:17799–802.
[6] Li W, Wang H, Yang T, Zhang H. Direct spectrometric determination of proteins in body fluids using a near-infrared cyanine dye. Analytical and Bioanalytical Chemistry 2003;377:350–5.
[7] Jisha V, Arun K, Hariharan M, Ramaiah D. Site-selective binding and dual mode recognition of serum albumin by a squaraine Dye. Journal of the American Chemical Society 2006;128:6024–5.
[8] Welder F, Paul B, Nakazumi H, Yagi S, Colyer C. Symmetric and asymmetric squarylium dyes as noncovalent protein labels: a study by fluorimetry and capillary electrophoresis. Journal of Chromatography B 2003; 793:93–105.
[9] Colyer C. Noncovalent labeling of proteins in capillary electrophoresis with laser-induced fluorescence detection. Cell Biochemistry and Biophysics 2000;33:323–37.
[10] Patonay G, Salon J, Sowell J, Strekowski L. Noncovalent labeling of biomolecules with red and near- infrared dyes. Molecules 2004;9:40–9.
[11] Denk W, Strickler J, Webb WW. Two-photon laser scanning fluorescence microscopy. Science 1990;248:73–6.
[12] So PTC, Dong CY, Masters BR, Berland KM. Two-photon excitation fluorescence microscopy. Annual Review of Biomedical Engineering 2000;2: 399–429.
[13] Jiang Y, Wang Y, Hua J, Qu S, Qian S, Tian H. Synthesis and two-Photon absorption properties of hyperbranched diketo-pyrrolo-pyrrole polymer with triphenylamine as the core. Journal of Polymer Science Part A: Polymer Chemistry 2009;47:4400–8.
[14] Jiang Y, Wang Y, Hua J, Tang J, Li B, Qian S, et al. Multibranched triarylamine end-capped triazines with aggregation-induced emission and larger two-photon absorption cross-sections. Chemical Communications 2010;46:4689–91.
[15] Xia Z, Su J, Fan H, Cheah K, Tian H, Chen C. Multifunctional diarylamine-substituted benzo[*k*]fluoranthene derivatives as Green Electroluminescent emitters and nonlinear optical materials. The Journal of Physical Chemistry C 2010;114:11602–6.
[16] Beverina L, Fu J, Leclercq A, Zojer E, Pacher P, Barlow S, et al. Two-photon absorption at telecommunications wavelengths in a dipolar chromophore with a pyrrole auxiliary donor and thiazole auxiliary acceptor. Journal of the American Chemical Society 2005;127:7282–3.
[17] Magennis S, Mackay F, Jones A, Tait K, Sadler P. two-photon-induced photoisomerization of an azo dye. Chemistry of Materials 2005;17:2059–62.
[18] Kim H, Cho B. Two-photon materials with large two-photon cross sections. Structure–property relationship. Chemical Communications; 2009:153–64.
[19] Huang C, Fan J, Peng X, Lin Z, Guo B, Cui J, et al. Highly selective and sensitive twin-cyano-stilbene-based two-photon fluorescent probe for mercury (ii) in aqueous solution with large two-photon absorption cross-section. Journal of Photochemistry and Photobiology A: Chemistry 2008;199:144–9.
[20] Dong X, Yang Y, Sun J, Liu Z, Liu B. Two-photon excited fluorescent probes for calcium based on internal charge transfer. Chemical Communications; 2009:3883–5.
[21] Eaton DF. International union of pure and applied chemistry organic chemistry division commission on photochemistry: reference materials for fluorescence measurement. Journal of Photochemistry and Photobiology B: Biology 1988;2(4):523–31.
[22] Xu C, Webb WW. Measurement of two-photon excitation cross sections of molecular fluorophores with data from 690 to 1050 nm. Journal of the Optical Society of America 1996;13:481–91.
[23] Wang J, Qian X. A series of polyamide receptor based PET fluorescent sensor molecules: positively cooperative Hg^{2+} ion binding with high sensitivity. Organic Letter 2006;8:3721–4.
[24] Wang J, Qian X, Cui J. Detecting Hg^{2+} ions with an ICT fluorescent sensor molecule: remarkable emission spectra shift and unique selectivity. The Journal of Organic Chemistry 2006;71:4308–11.
[25] Wenseleers W, Stellacci F, Meyer-Friedrichsen T, Mangel T, Bauer C, Pond S, et al. Five orders-of-magnitude enhancement of two-photon absorption for dyes on silver nanoparticle fractal clusters. The Journal of Physical Chemistry B 2002;106:6853–63.
[26] Basarić N, Baruah M, Qin W, Metten B, Smet M, Dehaen W, et al. Synthesis and spectroscopic characterization of BODIPY? Based fluorescent off-on indicators with low affinity for calcium. Organic & Biomolecular Chemistry 2005;3: 2755–61.
[27] Velapoldi RA, TÖnnesen HH. Corrected emission spectra and quantum yields for a series of fluorescent compounds in the visible spectral region. Journal of Fluorescence 2004;14:465–72.
[28] Armand F, Sakuragi H, Tokumaru K. Solvent effect on the charge-transfer transition of a novel amphiphilic pentacyano(4-octadecylaminopyridine)ferrate(III) complex. Journal of the Chemical Society, Faraday Transactions 1993;89:1021–4.
[29] Kim H, Jeong M, Ahn H, Jeon S, Cho B. Two-photon sensor for metal ions derived from azacrown ether. The Journal of Organic Chemistry 2004;69: 5749–51.
[30] Kim H, Kim B, Hong J, Park J, Lee K, Cho B. A two-photon fluorescent probe for calcium waves in living tissue. Angewandte Chemie International Edition 2007;46:7445–8.
[31] Kim H, Seo M, An M, Hong J, Tian Y, Lee K, et al. Two-photon fuorescent pobes for itracellular fee zinc ions in living tissue. Angewandte Chemie International Edition 2008;47:5167–70.
[32] Foster J. In albumin structure, function and uses. Oxford: Pergamon; 1977. pp. 53–84.